Research Article

Conditional Optimization on the Photocatalytic Degradation Removal Efficiency of Formaldehyde using TiO_2 – Nylon 6 Electrospun Composite Membrane

Taddao Pahasup-anan
International Program in Hazardous Substance and Environmental Management, Graduate School, Chulalongkorn University, Bangkok, Thailand
Center of Excellence on Hazardous Substance Management (HSM), Bangkok, Thailand

Kowit Suwannahong
School of Environmental Health, Faculty of Public Health, Burapha University, Chonburi, Thailand

Piyaporn Kampeerapappun
Faculty of Textile Industries, Rajamangala University of Technology Krungthep, Bangkok, Thailand

Ratthapol Rangkupan
Metallurgy and Materials Science Research Institute, Chulalongkorn University, Bangkok, Thailand

Wipada Dechapanya*
Department of Chemical Engineering, Faculty of Engineering, Ubon Ratchathani University, Ubonratchathani, Thailand

* Corresponding author. E-mail: wipada.d@ubu.ac.th DOI: 10.14416/j.asep.2024.07.012
Received: 5 May 2024; Revised: 8 June 2024; Accepted: 2 July 2024; Published online: 19 July 2024

Abstract
Since the outbreak of the coronavirus disease in 2019, many people have adjusted their work and lifestyle to the new normal, such as purchasing takeaway dishes or utilizing food delivery services more frequently. This causes individuals to spend more time indoors. The health, comfort, and well-being of building occupants are directly impacted by indoor air quality, which is a significant issue. The main objective of this study was to investigate the optimal conditions for the treatment of gaseous formaldehyde using TiO_2 – Nylon 6 electrospun composite membrane via photocatalytic oxidation. Response surface methodology (RSM) model with the Box-Behnken Design (BBD) was applied for experimental design and statistical analysis. Three factors (catalyst dosage, initial formaldehyde concentration, and gas flow rate) affecting the removal efficiency were studied. Three sets of experiments were conducted to compare the formaldehyde removal efficiencies of the following processes; the adsorption process, the photolysis process, and the photocatalytic oxidation process. From the results, it is obvious that the photocatalytic oxidation process yielded the highest removal efficiency (83.43%) as compared to the other two processes. The mechanism of the formaldehyde photocatalytic oxidation process can be described using the simplified Langmuir-Hinshelwood equation. The reaction follows a pseudo-first order reaction, with a rate constant of 0.0058 min^{-1}. The optimal conditions were found to be at 80.0%w/w catalyst dosage, 7.0 ppm initial formaldehyde concentration, and 1.5 L/min gas flow rate which resulted in an 84.54% removal efficiency after 420 minutes of treatment period. Thus, the application use of the TiO_2 – Nylon 6 electrospun composite membrane equipped with the UV light source could be a promising alternative technology for indoor air treatment.

Keywords: Electrospun membrane, Formaldehyde, Nylon 6, Photocatalytic oxidation, Response surface methodology, TiO_2

1 Introduction

During the coronavirus disease (COVID-19) pandemic, people worldwide have begun an adaptation process and are adhering to physical distancing requirements, which means staying home and away from others [1]. Due to lockdown orders, working from home has been one of the most significant and visible changes during the pandemic. Indoor air quality (IAQ) has become a major concern since people have spent more time indoors, generating more indoor air pollutants from indoor activities and prolonged exposure to those increases in indoor air emissions [2]. Poor IAQ can lead to a variety of health problems; for example, sick building syndrome (SBS), and building-related illness (BRI). SBS refers to acute health effects in which symptoms appear when humans live in buildings, but no cause can be identified, while BRI is health effects in which the cause of symptoms can be found [3]. Poor IAQ is caused by indoor air contaminants (IAC), which can be particulate matter (PM), smoke, biological agents (fungi, bacteria, spores, and pollen), gaseous contaminants, such as CO, CO_2, NO_2, Ozone, volatile organic compounds (VOCs) and formaldehyde [4]. Formaldehyde can be used as adhesive, sealants, resins, glues, and binders; and can be found in personal care products, plastic materials, paper manufacturing, various petrochemical processes and products, wood product manufacturing, and textiles, apparel, and leather. Thus, people are routinely exposed to formaldehyde in indoor air environments more or less. In addition, they are more exposed to formaldehyde if their homes are new or if there is new furniture since formaldehyde can be emitted at a high level from building products and furniture when newly formulated [5]. Many studies reported that exposure to indoor formaldehyde is associated with adverse health effects including asthma, bronchitis, conjunctivitis, dermatitis, ear infection, lung cancer, pneumonia, pregnancy outcome, and rhinitis [6]. Therefore, it is vital to remove these hazardous VOCs especially formaldehyde from the indoor environment.

One of the most highly promising methods used to purify indoor air quality is photocatalytic oxidation (PCO) technology [7]. PCO technology has been utilized to effectively reduce or eliminate several VOC species by converting organic compounds into water (H_2O) and carbon dioxide (CO_2). Removal of several VOCs has been studied and it was found that most of them can be completely destroyed [8]–[11]. For PCO effectiveness, photocatalyst particles need to be immobilized on a substrate surface to maintain photocatalytic activity throughout the operating life cycle [12]. Moreover, immobilizations help prevent the particles from detachment into the air stream and becoming air pollutants.

Simultaneous electrospinning electrospraying (SEE), a derivative of the electrospinning process, has been developed to immobilize nanoparticles (NPs) onto a polymer matrix. Particles were uniformly distributed inside the non-woven polymer membrane layer using the SEE method. The different voltage and feed flow rates were applied to control the deposition rate and film thickness [13]. There are several types of polymer used in the electrospinning process. Among them, nylon 6 with its chemical stability and mechanical strength gains more research attention for membrane utilization [14]. However, there have been few scientific publications on the use of the SEE method to immobilize photocatalysts for PCO applications, particularly for indoor air purification. In addition, the design of a PCO air purification system is complicated due to various process parameters [7]. Therefore, the Response Surface Methodology (RSM) was used to optimize the operation parameters of a photocatalytic process using PCMs to predict the maximum formaldehyde degradation rate under constraint conditions. The potential use of TiO_2 – nylon 6 photocatalytic composite membranes (PCM) as an air purifier was evaluated for photocatalytic activity on formaldehyde degradation in a closed-air recirculation system as well.

2 Materials and Methods

2.1 *Fabrication of PCM membrane*

Based on our previous study, simultaneous electrospinning and electrospraying were performed [15]. Solution of Nylon 6 and dispersed Anatase-TiO_2 in absolute ethanol was electrospun and electrosprayed at a steady rate through a needle linked to a high-voltage power source. The positive and negative polarities were exploited for the electrospinning and the electrospraying, respectively. To collect the prepared membrane, a rotating metal drum with a constant speed was applied in this process. The PCM was generated by electrospinning nylon 6 for 15 minutes to create a base layer, followed by simultaneous electrospinning and electrospraying of both materials for four hours. To avoid TiO_2

agglomeration, the dispersed TiO_2 was replaced every 2 h. Lastly, nylon 6 was electrospun for another 15 min on the top layer of PCM to avoid the loss of TiO_2 from the membrane. The produced PCM was dried at room temperature overnight before being stored in an electronic desiccator for subsequent testing.

2.2 *Formaldehyde degradation via photocatalytic oxidation*

The photocatalytic process was developed as a closed-air recirculation system as shown in Figure 1. The system is divided into two parts: the pollution chamber and the photocatalytic reactor. The pollution chamber was composed of glass to reduce pollutant adsorption inside. An electrical fan was installed inside the chamber to evaporate the pollutant and allow for complete mixing, as well as a carbon dioxide sensor to measure carbon dioxide produced by the photocatalytic reaction and a temperature and humidity sensor to monitor temperature and humidity during the experiment.

For the photocatalytic reactor, a 7-watt UV-C lamp (SOBO, China) was equipped at the center of the reactor and served as the reaction's energy source. The distance between the light bulb and the membrane was set at 25 mm resulting in a light intensity of about 9.5 mW/cm^2. The photocatalytic activities of one sheet of the membrane with a total surface area of 150 cm^2 were investigated.

Before being used, the pollution chamber was cleansed with fresh dry air. The desired amount of formaldehyde solution was injected into the chamber by turning on the electrical fan to generate formaldehyde vapor [16], [17]. The concentration of formaldehyde after evaporation was recorded using the formaldehyde meter (HAL-HFX205, Hal Technology, USA) and utilized as the initial concentration value. Then, the formaldehyde vapor was pumped into the photocatalytic reactor to start the reaction. The concentration of formaldehyde was measured every 2 min throughout 420 min of the test after turning on the UV-C lamp at a temperature of 25 °C. To confirm the photocatalytic reaction, The CO_2 concentration in the pollution chamber was monitored using a CO_2 meter (Lutron MCH-388SD, Lutron Electric Enterprise, Taiwan).

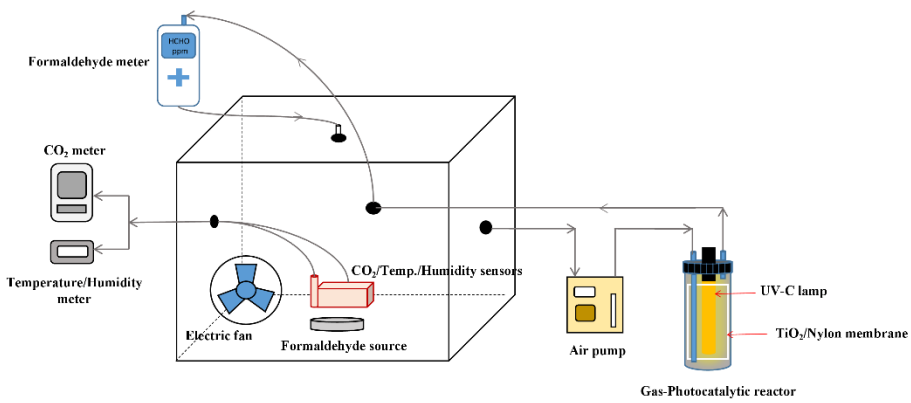

Figure 1: Schematic diagram of photocatalytic degradation of formaldehyde.

2.3 *Kinetic Study*

The Langmuir–Hinshelwood (L–H) equation (Equation 1) is a widely accepted equation used to describe the photocatalytic oxidation mechanism, which includes the adsorption of reactants onto the photocatalyst surface. The L–H model has been widely used for VOC catalytic reaction rate equations [16], [18]–[20]. In addition, the pseudo-first-order kinetics or simplified L-H form has been used for fitting the degradation process at low concentrations of the pollutant [20], [21].

$$-dC/dt = kKC/(1+KC) \quad (1)$$

Where k is the reaction rate constant, K is the adsorption equilibrium constant, t is the retention time, and C is the pollutant concentration. If the pollutant concentration is dilute, the L-H equation could be simplified as a pseudo-first-order reaction (Equation (2)).

$$\ln(C_o/C) = kKt = k't \quad (2)$$

where k' is the reaction rate constant and C_o is the initial pollutant concentration.

2.4 *Photocatalytic process optimization*

Response Surface Methodology (RSM) technique was used to optimize the formaldehyde removal efficiency affected by the photocatalytic parameters including catalyst dosage, initial formaldehyde concentration, and air flow rate. The optimization process began with the selection of an experiment design (DOE). The DOE, Box-Behnken Design (BBD) was used to create an experiment for the three parameters which were selected as independent parameters. The removal efficiency of formaldehyde was the output response or dependent parameter. Table 1 shows the ranges and levels of the independent parameters and the dependent parameter for the BBD experimental design.

Table 1: Independent variables and their levels for the Box-Behnken experimental design.

Independent Variables (Factors)	Level used		
	Low (–1)	Medium (0)	High (+1)
A = Catalyst dosage (%w/w)	40	60	80
B = Initial concentration (ppm)	3	5	7
C = Flow rate (L/min)	0.5	1	1.5
Dependent variable (response)			
Y = Removal efficiency (%)	Maximize		

The model included three experimental components with three levels of each parameter. The model provided the results of 15 runs of experiments, including three replications at the central location. All experiments were carried out in duplicate and analyzed by the analysis of variance (ANOVA) at 95% confidence. Three-dimensional response surface analysis of the independent and dependent parameters was used to estimate the optimal values of the parameters. The RSM, statistical analysis, and optimization process were performed by using the Design Expert (Trial Version 13).

3 Results and Discussion

3.1 *Morphological Assessment of PCM*

The PCM morphology before and after one cycle of PCO treatment is shown in Figure 2.

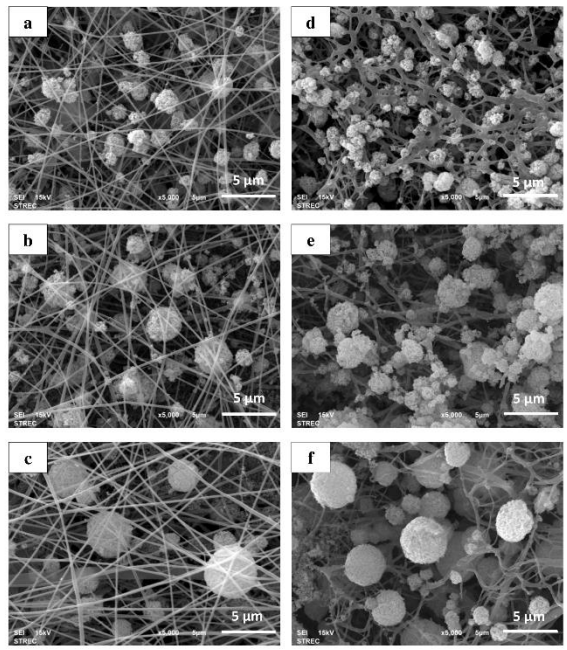

Figure 2: SEM micrographs of as prepared PCM: PCM with TiO_2 40 %w/w (a); PCM with TiO_2 60 %w/w (b); PCM with TiO_2 80 %w/w (c), and the membrane after one cycle of PCO treatment: PCM with TiO_2 40 %w/w (d); PCM with TiO_2 60 %w/w (e); PCM with TiO_2 80 %w/w(f).

Figure 2(a)–(c), represents the morphology of the PCM before usage. As can be seen, TiO_2 microclusters were entrapped within fibrous layers. After one treatment cycle (Figure 2(d)–(f)), it was clear that the appearance of polymer fibrous structures in all samples exhibited fiber breakage, leaving TiO_2 microclusters loosely attached to the top layer of the PCM membrane. However, the TiO_2 microclusters were maintained in a spherical shape without any deformation as shown in SEM images. The fiber breakage most likely was the result of UV irradiation. This finding implies that the microcluster entrapment would be preserved as long as the fibrous network's integrity could be maintained. As a result, improving PCM durability under UV light could be a promising area for further research. Based on visual inspection, all PCMs appear to be slightly thinner and partially torn in random areas that agree with SEM results.

3.2 *Photocatalytic degradation of formaldehyde*

The formaldehyde degradation resulted in a slight increase in formaldehyde degradation when the

catalyst dosage was increased (Figure 3(a)). The amount of photocatalyst can affect the photocatalytic oxidation process by altering the generation rate of electron-hole pairs [16]. When the amount of TiO_2 is raised, the photocatalyst can absorb more photons, resulting in more electron-hole pairs being formed, leading to more formaldehyde breakdown [22]. When the initial formaldehyde concentration increased from 3 to 7 ppm, the formaldehyde degradation increased (Figure 3(b)). The efficiency of formaldehyde removal was improved by increasing the initial formaldehyde concentration since the more amount of formaldehyde molecules were adsorbed onto the photocatalyst surface at the elevated concentration of initial formaldehyde concentration, resulting in a good oxidation reaction of hydroxyl radicals and formaldehyde, and thus an increase in formaldehyde degradation rate [23].

Adjusting the gas flow rate from 0.5 to 1.5 L/min could affect the PCO by changing the convection mass transfer and the adsorption of formaldehyde molecules on the photocatalyst surface [16]. Three different gas flow rates were tested including 0.5, 1.0, and 1.5 L/min resulting in residence time of 84.78, 42.39, and 28.26 s and Reynolds number (Re) of 29.32, 58.64, and 87.95, respectively (Figure 3(c)). The calculated Re indicated all measured flow rates provided a laminar flow process.

The photocatalytic breakdown of gaseous molecules could take place via two mechanisms: direct oxidation on the photocatalyst surface (heterogeneous reaction) and oxidation near the boundary layer (BL) or in the bulk phase (homogeneous reaction). Increasing the gas flow rate improved mixing in the reactor, which aided interface mass transfer by increasing the mobility of radicals generated on the photocatalyst surface to the boundary layer, encouraging oxidation in the boundary layer or the bulk phase. As a result, raising the gas flow rate resulted in increased formaldehyde degradation as a result of oxidation occurring not only on the photocatalyst surface but also in the bulk phase [24].

3.2 *Comparison between adsorption, photolysis, and photocatalysis*

The degradation of formaldehyde was investigated at the initial concentration of 5 ppm and the air flow rate of 1 L/min for the three processes namely adsorption, photolysis, and photocatalysis. For the adsorption process, the PCM using the PCM with 60 %w/w of TiO_2 was evaluated for its adsorption efficiency. The UV light source with a light intensity of 9.5 mW/cm^2 was applied for the investigation of formaldehyde decomposition via photolysis. The formaldehyde degradation using the PCM with 60 %w/w of TiO_2 via photocatalytic process was examined at different UV light intensities. The removal efficiencies of formaldehyde after 420 min of experimental time frame for adsorption, photolysis, and photocatalysis were approximately 39.25%, 38.50%, and 78.23%, respectively. As can be observed the removal efficiencies of adsorption and photolysis are relatively low as compared to that of photocatalysis. The efficiency of gaseous adsorption depends on both the pore structures and surface properties of adsorbent materials [25]. The photolysis test removed the lowest amount of formaldehyde because the UV intensity used was insufficient to eliminate formaldehyde without the addition of a TiO_2 photocatalyst [26]. The combination of a UV light source and photocatalytic material resulted in more formaldehyde degradation via photocatalysis. TiO_2 in the PCM was activated by UV light and released the reactive species OH• and O_2 from the oxidation and reduction on the photocatalyst surface respectively. The OH• radical plays an important role in the oxidation of gaseous formaldehyde adsorbed on the photocatalyst surface and its conversion to harmless CO_2 and water. Formaldehyde decomposition increases with UV irradiation in direct proportion to formaldehyde adsorption. The mesoporous structure of the PCM can enhance the degradation ability because it has a large pore volume, which improves the capability for formaldehyde adsorption [25].

The production of CO_2 was measured to confirm the photocatalytic reaction. The average CO_2 concentration increases from 360 ppm to 500 ppm in Figure 4(c). The correlation between a rise in CO_2 content and a decrease in formaldehyde demonstrates that gaseous formaldehyde is degraded via the PCO process. As indicated in Figure 4(a), the CO_2 concentration throughout adsorption was nearly constant. This result demonstrated that no CO_2 was produced in the adsorption process. The products generated in the reactions of formaldehyde photolysis include HCO and CO. The reaction mechanism of formaldehyde photolysis showed that monitoring CO_2 production in formaldehyde photolysis would be impossible, as shown in Figure 4(b).

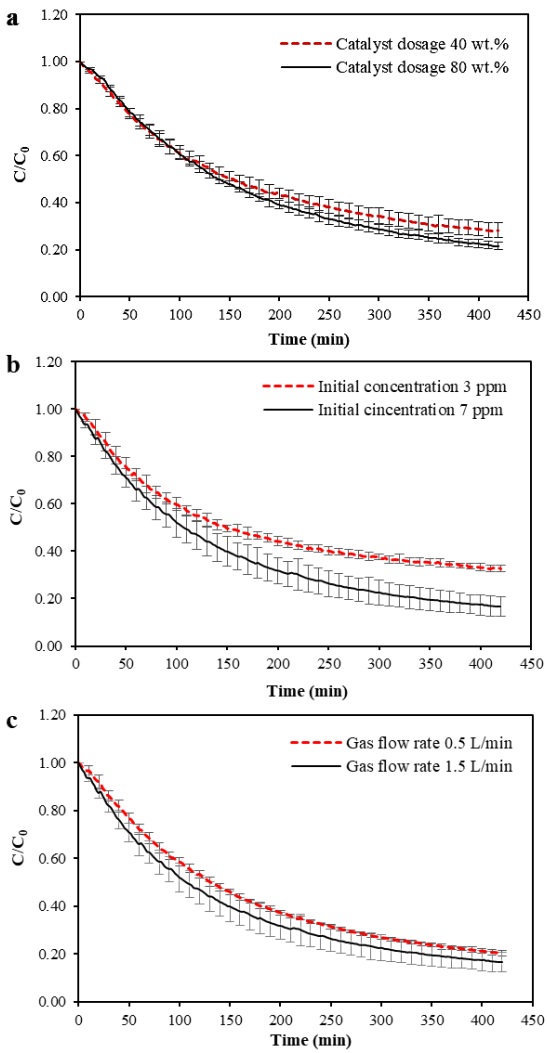

Figure 3: Effect of catalyst dosage (a); initial formaldehyde concentration (b); volumetric gas flow rate (c) on the degradation of formaldehyde.

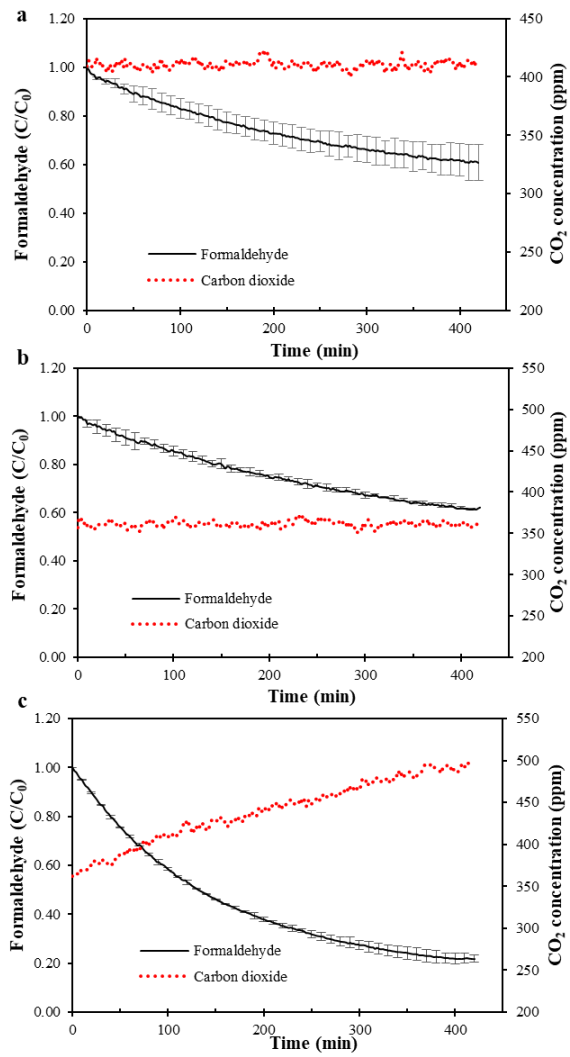

Figure 4: The degradation of formaldehyde by: adsorption (a); photolysis (b); photocatalysis (c).

3.4 *Kinetics Study*

The kinetic parameter (k') retrieved from a result of the natural logarithm of the normalized formaldehyde concentration vs time (Equation 2) for the degradation process under optimal conditions, a good fit of the actual data to the model with R^2 equal to 0.9936, and the apparent reaction rate determined from the graph is 0.0058 min^{-1} [27].

3.5 *Statistical Analysis*

The photocatalytic degradation of formaldehyde was conducted using the Box–Behnken Design, with a total of 15 experimental runs. Table 2 shows that the removal efficiency with a treatment time of 420 minutes ranged from 62.04 to 83.43%. The lowest removal efficiency (62.04%) was obtained when using the PCM with a catalyst dosage of 60% w/w, an initial concentration of 3 ppm, and an air flow rate of 0.5 L/min. The highest removal efficiency (83.43%) received was at the catalyst dosage of 60% w/w, the initial concentration of 7 ppm, and the flow rate of 1.5 L/min. Results in Table 2 indicate that removal

efficiency was significantly affected by initial concentration in which removal efficiency increases with initial concentration as described in Section 3.2. As demonstrated in Table 2, the empirical model's predicted removal efficiencies are in good agreement with those obtained from experiments.

The fitness of the model was verified by regression model analysis and the analysis of variance (ANOVA). The coefficient of determination (R^2) is a number indicating the degree of fit; if R^2 is close to 1, the model fits well with the actual data. In this study, the R^2 value of the proposed model is 0.9265, which is greater than 0.8 as shown in Table 3. The Predicted R^2 of 0.6377 is in reasonable agreement with the Adjusted R^2 of 0.7943 (the difference is less than 0.2). Adequacy precision measures the signal-to-noise ratio. A ratio greater than 4 is desirable. The ratio of 7.883 indicates an adequate signal [28]. In addition, the coefficient of variation (CV) is less than 10%. Thus, the model can be used to navigate the design space [29].

Table 2: Comparison of experimental and predicted removal efficiencies.

Run	Experimental Factors			Removal Efficiency (%)	
	Catalyst Dosage (%w/w)	Initial Concentration (ppm)	Flow Rate (L/min)	Experiment	Predicted
1	40	3	1.0	64.29 ± 2.34	62.94
2	40	5	0.5	71.67 ± 3.01	71.87
3	40	5	1.5	75.90 ± 0.83	76.98
4	40	7	1.0	78.29 ± 0.80	78.36
5	60	3	0.5	62.04 ± 9.37	63.19
6	60	3	1.5	67.29 ± 1.40	67.56
7	60	7	0.5	79.78 ± 1.13	79.51
8	60	5	1.0	73.43 ± 1.15	73.78
9	60	5	1.0	78.23 ± 1.50	73.78
10	60	5	1.0	69.69 ± 1.30	73.78
11	60	7	1.5	83.43 ± 4.15	82.28
12	80	3	1.0	66.81 ± 0.19	66.74
13	80	5	0.5	78.40 ± 1.54	77.32
14	80	5	1.5	79.55 ± 0.91	79.35
15	80	7	1.0	81.01 ± 1.02	82.36

Table 3: RSM model summary of statistics parameters for formaldehyde removal.

Std. Dev.	Mean	C.V. %	Adequacy Precision	R^2	Adjusted R^2	Predicted R^2
3.02	73.99	4.08	7.8833	0.9265	0.7943	0.6377

The ANOVA was used to examine the model significance, and the results are displayed in Table 4. The model has an *F*-value of 7.01, indicating that it is significant with only a 2.26% chance that the value could occur due to noise. The p-value of the model is 0.0266, which is less than 0.0500 confirming that the model is highly significant. The lack of fit F-value of 0.1616 implies that the lack of fit is not significant relative to the pure error. While the lack of fit p-value is 0.9138, which is greater than 0.05, the non-significant lack of fit also supports the good fitness of the model [30]. Overall, statistical analysis revealed that the experimental data were accurate and reliable in fitting the model [31]. Furthermore, most of the *p*-values of each term expressed in the model are higher than 0.05 except for the initial concentration of formaldehyde (B) having a p-value of 0.0008 indicating that this factor has a statistically significant effect on the removal efficiency. The finding of this research agrees well with others [32], [33]. The results from ANOVA suggested that the catalyst dosage and air flow rate having a p-value of less than 0.05 have no significant effect on the photocatalytic destruction of formaldehyde in the studied ranges. This may be implied that there is a sufficient amount of TiO_2 to react with formaldehyde molecules at 40%–80% w/w. Also, the retention time for the destruction of gaseous formaldehyde in the ranges of 0.5–1.5 L/min air flow rate was enough for the photocatalytic reaction to occur. Therefore, these two parameters have an insignificant impact on the photocatalytic destruction of formaldehyde.

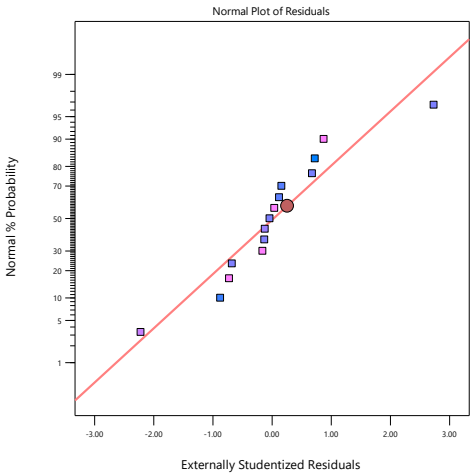

Figure 5: Normal percent probability of residuals versus externally studentized residuals of formaldehyde removal efficiency.

Figure 5 demonstrates the normal percent probability and externally studentized residuals. As can be seen, any apparent problems with the normal probability plot could not be observed. A good correlation between input and output variables can be derived from the empirical model [30]. Moreover, residuals scattering along a straight line assure the normality assumption suggesting good agreement between the experimental and predicted values [28].

Model fitting by Design Expert software was used to obtain the best-fitted model with the purpose of the formaldehyde degradation process optimization. The empirical linear equation was derived from the fitting experimental data and stated in terms of actual elements as follows:

$$y = 40.413125 - 0.140875A + 9.7404167B - 2.3367C + 0.00125AB - 0.077AC - 0.4BC + 0.002577083A^2 - 0.55354167B^2 + 6.26333C^2 \quad (3)$$

where y is the removal efficiency (%), A is the terms of coded value for catalyst dosage (%w/w), B is the terms of coded value for initial formaldehyde concentration (ppm), and C is the terms of coded value for gas flow rate (L/min).

The model validation was carried out to ensure the accuracy of the mathematical model received from the BBD for the prediction of removal efficiency. Results in Table 5 show a reasonable agreement between the experimental and predicted data. Thus, it could be concluded that the model, as shown in Equation (3), can be successfully used to predict formaldehyde removal efficiency via photocatalytic degradation.

Table 4: Analysis of variance (ANOVA) for the response surface model.

Source	Sum of Squares	df	Mean Square	*F*-value	*p*-value	Remark
Model	574.38	9	63.82	7.01	0.0266	Significant
A: Catalyst dosage	30.50	1	30.50	3.35	0.1268	
B: Initial concentration	481.74	1	481.74	52.90	0.0008	
C: Gas flow rate	25.49	1	25.49	2.80	0.1552	
AB	0.0010	1	0.0010	0.0011	0.9748	
AC	2.37	1	2.37	0.2604	0.6316	
BC	0.6400	1	0.6400	0.0703	0.8015	
A^2	3.92	1	3.92	0.4308	0.5406	
B^2	18.10	1	18.10	1.99	0.2177	
C^2	9.05	1	9.05	0.9940	0.3645	
Residual	45.54	5	9.11			
Lack of fit	8.88	3	2.96	0.1616	0.9138	Not significant
Pure Error	36.65	2	18.33			
Total	619.92	14				

Table 5: Validation of mathematical model received from RSM for formaldehyde removal.

Experimental Factors			Removal Efficiency (%)		
Catalyst Dosage (%w/w)	Initial Concentration (ppm)	Flow Rate (L/min)	Experiment	Model	Error (%)
40	3	1.0	62.63	62.94	0.48
40	5	1.5	75.31	76.98	0.77
60	3	0.5	68.66	63.19	2.22
60	5	1.0	74.25	73.78	1.06
60	7	0.5	80.59	79.51	7.97
80	5	1.5	80.20	79.35	1.34
80	7	1.0	81.73	82.36	0.63

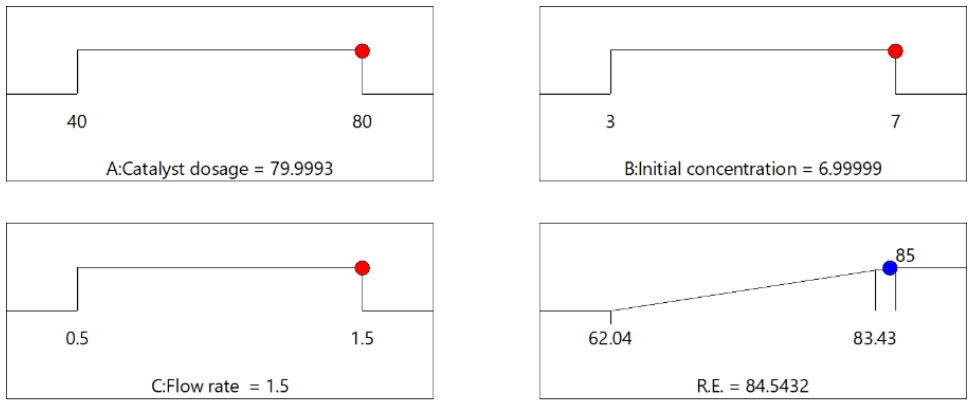

Figure 6: Numerical optimization of process variables for formaldehyde removal.

Table 6: Verification for Optimal conditions.

Parameter	Model Conditions	Experimental Conditions	Removal Efficiency (%)	
			Predicted	Experiment
Catalyst dosage (%w/w)	80.0	80.8	84.54	83.26 ± 3.39
Initial concentration (ppm)	7.00	7.12		
Gas flow rate (L/min)	1.50	1.50		

3.6 *Optimal condition and validation*

The optimal conditions for the formaldehyde removal efficiency by photocatalytic oxidation were investigated and accomplished using the response optimizer function in a statistical package. The optimal conditions were chosen with the highest value of the composite desirability (D) function, which has a value between 0–1. If the D value is equal to 1, then the result is completely satisfied [31]. The optimal criteria set for the maximum removal efficiency target in the software were as follows: lowest and highest values of catalyst dosage, initial concentration, and air flow rate are 20% and 80% w/w, 3 and 7 ppm, and 0.5 and 1.5 L/min, respectively. From the response optimizer results, 68 conditions were derived from the model, however, the optimal conditions suggested by the model were at the catalyst dosage of 80.0 %w/w, the initial formaldehyde concentration of 7 ppm, and gas flow rate of 1.5 L/min as shown in Figure 6. Since these conditions yield a formaldehyde removal efficiency of 84.5432% and a D value of 0.980.

A set of experiments (triplet runs) was conducted to confirm the optimal conditions received from the RSM. As seen from Table 6, the average value of formaldehyde removal efficiency obtained from the experiment was 83.26%, which is in good agreement with that of the model (84.54%). This result confirms the great appropriateness of the model for the optimization of formaldehyde removal via photocatalytic oxidation.

A three-dimensional surface diagram is a graphical representation of the regression equation that can be used to optimize the parameters and examine the interactions between them [29]. The interaction effects between the three independent parameters and the dependent parameter are displayed in Figure 7. Figure 7(a) shows the interaction effect of catalyst dosage and initial formaldehyde concentration on formaldehyde removal efficiency depicted in a linear response surface graph. The PCM with the highest catalyst dosage and initial formaldehyde concentration produced the highest formaldehyde removal efficiency. The effect of catalyst dosage on the photocatalytic degradation of formaldehyde was not significant for any constant value of initial formaldehyde concentration in the range of 3 to 7 ppm.

The interaction effect of initial formaldehyde concentration and gas flow rate on the formaldehyde removal efficiency depicted a linear curve shown in Figure 7(b). The highest initial formaldehyde concentration and gas flow rate resulted in the highest formaldehyde removal efficiency. At any constant value of gas flow rate in the range of 0.5 to 1.5 L/min, the effectiveness of formaldehyde removal improves dramatically with rising initial formaldehyde concentration. However, at any initial formaldehyde concentration between 3 and 7 ppm, the formaldehyde removal efficiency slightly increases with the increasing gas flow rate value, thus the change in gas flow rate has no appreciable impact on the percentage

of formaldehyde degradation. The effect of gas flow rate and catalyst dosage on the formaldehyde removal efficiency is shown in Figure 7(c). It is clear that the interaction effect of gas flow rate and catalyst dosage has no significant effect on the formaldehyde removal efficiency. From the optimization results, it is emphasized that the PCM with a UV light source could be applied for indoor air purifiers, especially at high levels of gaseous formaldehyde.

4 Conclusions

After 420 min of experimental time, the PCMs demonstrated effective decomposition of gaseous formaldehyde, with removal efficiencies ranging from 62.04% to 83.43%. The response surface methodology (RSM) with the Box–Behnken Design can produce statistically accurate findings for estimating the effect of catalyst dosage, initial formaldehyde concentration, and gas flow rate on formaldehyde degradation via the PCO process. The RSM could be applied for optimization of formaldehyde removal efficiency using the PCM. The optimal conditions obtained from the model under the related constraints were evaluated to be 80 %w/w of catalyst dosage, 7 ppm of initial formaldehyde concentration, and 1.50 L/min of volumetric gas flow rate with 84.54% formaldehyde removal efficiency. The L – H kinetic model confirmed the surface reaction on the photocatalytic material which the obtained reaction rate (k') was 0.0058 min-1. The finding of this research indicates that the PCM can be further developed and synthesized for use as a highly active air purifier with a suitable UV light source for residential, commercial, and industrial buildings.

Acknowledgments

This research was supportably funded by the 90th Anniversary of Chulalongkorn University, Rachadapisek Sompote Fund, The International Program in Hazardous Substance and Environmental Management, Graduate School, Chulalongkorn University, the Environmental Management Center of Excellence on Hazardous Substance Management (HSM), Chulalongkorn University and the Second Century Fund, Chulalongkorn University.

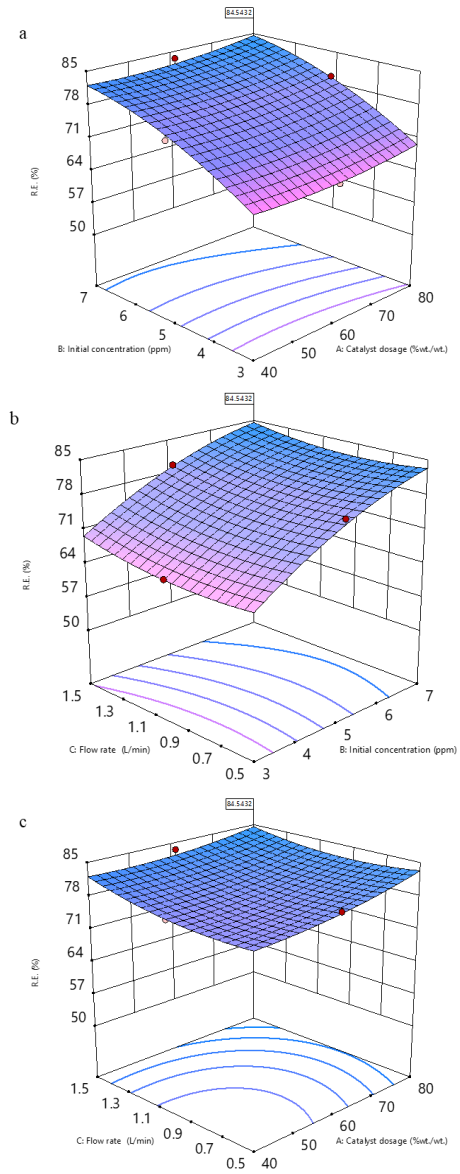

Figure 7: Response surface 3D plot demonstrates the interaction effect of catalyst dosage and initial formaldehyde concentration (a); initial formaldehyde concentration and gas flow rate (b); and gas flow rate and catalyst dosage (c) on formaldehyde removal efficiency.

Author Contributions

T.P.: conceptualization, investigation, reviewing, data analysis, editing, and funding acquisition; K.S.: conceptualization; P.K.: writing an original draft; R.R.: conceptualization, editing, and funding acquisition; W.D.: research design, methodology, data curation, writing—reviewing, editing, data analysis, and project administration. All authors have read and agreed to the published version of the manuscript.

Conflicts of Interest

The authors declare no conflict of interest.

References

[1] S. N. Saleh, C. U. Lehmann, S. A. McDonald, M. A. Basit, and R. J. Medford, "Understanding public perception of coronavirus disease 2019 (COVID-19) social distancing on Twitter," *Infection Control & Hospital Epidemiology*, vol. 42, no. 2, pp. 131–138, Aug. 2021, doi: 10.1017/ice.2020.406.

[2] M. Somani, A. N. Srivastava, S. K. Gummadivalli, and A. Sharma, "Indirect implications of COVID-19 towards sustainable environment: An investigation in Indian context," *Bioresource Technology Reports*, vol. 11, Sep. 2020, Art. no. 100491, doi: 10.1016/j.biteb.2020.100491.

[3] EPA, "Indoor Air Facts No.4 (revised) Sick Building Syndrome," EPA, OH, 1991.

[4] T. M. Mata, F. Felgueiras, A. A. Martins, H. Monteiro, M. P. Ferraz, G. M. Oliveira, M. F. Gabriel, and G. V. Silva, "Indoor air quality in elderly centers: Pollutants emission and health effects," *Environments*, vol. 9, no.7, p. 86, Jul. 2022, doi: 10.3390/environments9070086.

[5] EPA, "Risk evaluation for formaldehyde," 2024. [Online]. Available: https://www.epa.gov/assessing-and-managing-chemicals-under-tsca/risk-evaluation-formaldehyde#:~:text=Due%20to%20its%20varied%20sources%2C%20people%20are%20routinely,and%20if%20it%20is%20absorbed%20into%20the%20skin

[6] N. Liu, L. Fang, W. Liu, H. Kan, Z. Zhao, F. Deng, C. Huang, B. Zhao, X. Zeng, Y. Sun, H. Qian, J. Mo, C. Sun, J. Guo, X. Zheng, Z. Bu, L. B. Weschler, and Y. Zhang, "Health effects of exposure to indoor formaldehyde in civil buildings: A systematic review and meta-analysis on the literature in the past 40 years," *Building and Environment*, vol. 233, Apr. 2023, Art. no. 110080, doi: 10.1016/j.buildenv.2023.110080.

[7] T. M. Mata, A. A. Martins, C. S. C. Calheiros, F. Villanueva, N. P. Alonso-Cuevilla, M. F. Gabriel, and G. V. Silva, "Indoor air quality: A review of cleaning technologies," *Environments*, vol. 9, no. 9, Sep. 2022, doi: 10.3390/environments9090118.

[8] A. E. Cassano and O. M. Alfano, "Reaction engineering of suspended solid heterogeneous photocatalytic reactors," *Catalysis Today*, vol. 58, no. 2, pp. 167–197, May 2000, doi: 10.1016/S0920-5861(00)00251-0.

[9] V. Héquet, C. Raillard, O. Debono, F. Thévenet, N. Locoge, and L. Le Coq, "Photocatalytic oxidation of VOCs at ppb level using a closed-loop reactor: The mixture effect," *Applied Catalysis B: Environmental*, vol. 226, pp. 473–486, Jun. 2018, doi: 0.1016/j.apcatb.2017.12.041.

[10] J. Sydorenko, A. Mere, M. Krunks, M. Krichevskaya, and I.O. Acik, "Transparent TiO_2 thin films with high photocatalytic activity for indoor air purification," *RSC Advances*, vol. 12, no. 55, pp. 35531–35542, Dec. 2022, doi: 10.1039/D2RA06488J.

[11] E. Tapia-Brito, J. Riffat, Y. Wang, Y. Wang, A. M. Ghaemmaghami, C. M. Coleman, M.T. Erdinç, and S. Riffat, "Experimental study of the purification performance of a MopFan-based photocatalytic air cleaning system," *Building and Environment*, vol. 240, Jul. 2023, Art. no. 110422, doi: 10.1016/j.buildenv.2023.110422.

[12] Z. Han, V. W. C. Chang, L. Zhang, M. S. Tse, O. K. Tan, and L. M. Hildemann, "Preparation of TiO_2-coated polyester fiber filter by spray-coating and its photocatalytic degradation of gaseous formaldehyde," *Aerosol and Air Quality Research*, vol. 12, no. 6, pp. 1327–1335, Dec. 2012, doi: 10.4209/aaqr.2012.05.0114.

[13] A. Jaworek and A. T. Sobczyk, "Electrospraying route to nanotechnology: An overview," *Journal of Electrostatics*, vol. 66, no. 3–4, pp. 197–219, Mar. 2008, doi: 10.1016/j.elstat.2007.10.001.

[14] M. G. Ali, H. M. Mousa, F. Blaudez, M. S. Abd El-sadek, M. A. Mohamed, G. T. Abdel-Jaber, A. Abdal-hay, and S. Ivanovski, "Dual nanofiber

scaffolds composed of polyurethane-gelatin/nylon 6- gelatin for bone tissue engineering," *Colloids and Surfaces A: Physicochemical and Engineering Aspects*, vol. 597, Jul. 2020, Art. no. 124817, doi: 10.1016 /j.colsurfa.2020.124817.

[15] T. Pahasup-anan, K. Suwannahong, W. Dechapanya, and R. Rangkupan, "Fabrication and photocatalytic activity of TiO_2 composite membranes via simultaneous electrospinning and electrospraying process," *Journal of Environmental Sciences (China)*, vol. 72, pp. 13–24, Oct. 2018, doi: 10.1016/j.jes.2017.11.025.

[16] Z. Han, V.-W. Chang, X. Wang, T.-T. Lim, and L. Hildemann, "Experimental study on visible-light induced photocatalytic oxidation of gaseous formaldehyde by polyester fiber supported photocatalysts," *Chemical Engineering Journal*, vol. 218, pp. 9–18, Feb. 2013, doi: 10.1016/ j.cej.2012.12.025.

[17] S. B. Kim and S. C. Hong, "Kinetic study for photocatalytic degradation of volatile organic compounds in air using thin film TiO_2 photocatalyst," *Applied Catalysis B: Environmental*, vol. 35, no. 4, pp. 305–315, Jan. 2002, doi: 10.1016/S0926-3373(01)00274-0.

[18] C. H. Ao, S. C. Lee, J. Z. Yu, and J. H. Xu, "Photodegradation of formaldehyde by photocatalyst TiO_2: Effects on the presences of NO, SO2 and VOCs," *Applied Catalysis B: Environmental*, vol. 54, no. 1, pp. 41–50, Nov. 2004, doi: 10.1016/j.apcatb.2004.06.004.

[19] H. Qi, D.-z. Sun, and G.-q. Chi, "Formaldehyde degradation by UV/TiO_2/O_3 process using continuous flow mode," *Journal of Environmental Sciences*, vol. 19, no. 9, pp. 1136–1140, Jan. 2007, doi: 10.1016/S1001-0742(07)60185-5.

[20] G. Zhang, Z. Sun, Y. Duan, R. Ma, and S. Zheng, "Synthesis of nano-TiO_2/diatomite composite and its photocatalytic degradation of gaseous formaldehyde," *Applied Surface Science*, vol. 412, pp. 105–112, Aug. 2017, doi: 10.1016/ j.apsusc.2017.03.198.

[21] C. Si, J. Zhou, H. Gao, and G. Liu, "Photocatalytic degradation of formaldehyde in a fluidized bed with sound-magnetic assistance," *Advanced Powder Technology*, vol. 24, no. 1, pp. 295–300, Jan. 2013, doi: 10.1016/j.apt.2012.07.005.

[22] G. Zhang, Z. Sun, X. Hu, A. Song, and S. Zheng, "Synthesis of BiOCl/TiO_2–zeolite composite with enhanced visible light photoactivity," *Journal of the Taiwan Institute of Chemical Engineers*, vol. 81, pp. 435–444, Dec. 2017, doi: 10.1016/j.jtice.2017.09.030.

[23] M.T. Laciste, M.D.G. de Luna, N.C. Tolosa, and M.-C. Lu, "Degradation of gaseous formaldehyde via visible light photocatalysis using multi-element doped titania nanoparticles," *Chemosphere*, vol. 182, pp. 174–182, Sep. 2017, doi: 10.1016/ j.chemosphere.2017.05.022.

[24] B. M. da Costa Filho, A. L. P. Araujo, G. V. Silva, R. A. R. Boaventura, M. M. Dias, J. C. B. Lopes, and V. J. P. Vilar, "Intensification of heterogeneous TiO_2 photocatalysis using an innovative micro-meso-structured-photoreactor for n-decane oxidation at gas phase," *Chemical Engineering Journal*, vol. 310, pp. 331–341, Feb. 2017, doi: 10.1016/j.cej.2016.09.080.

[25] J. Ji, Y. Xu, H. Huang, M. He, S. Liu, G. Liu, R. Xie, Q. Feng, Y. Shu, Y. Zhan, R. Fang, X. Ye, and D.Y.C. Leung, "Mesoporous TiO_2 under VUV irradiation: Enhanced photocatalytic oxidation for VOCs degradation at room temperature," *Chemical Engineering Journal*, vol. 327, pp. 490–499, Nov. 2017, doi: 10.1016/j.cej.2017.06.130.

[26] T. N. Obee and R. T. Brown, "TiO_2 photocatalysis for indoor air applications: effects of humidity and trace contaminant levels on the oxidation rates of formaldehyde, toluene, and 1,3-Butadiene," *Environmental Science & Technol*ogy, vol. 29, no. 5, pp. 1223–1231, May 1995, doi: 10.1021/es00005a013.

[27] H. Liu, Z. Lian, X. Ye, and W. Shangguan, "Kinetic analysis of photocatalytic oxidation of gas-phase formaldehyde over titanium dioxide," *Chemosphere*, vol. 60, no. 5, pp. 630–635, Jun. 2005, doi: 10.1016/j.chemosphere.2005.01.039.

[28] A. Hamisu, U. I. Gaya, and A. H. Abdullah, "Bi-template assisted sol-gel synthesis of photocatalytically-active mesoporous anatase TiO_2 nanoparticles," *Applied Science and Engineering Progress*, vol. 4, no. 3, pp. 313–327, 2021, doi: 10.14416/j.asep.2021.04.003.

[29] J. Zhang, D. Fu, Y. Xu, and C. Liu, "Optimization of parameters on photocatalytic degradation of chloramphenicol using TiO_2 as photocatalyst by response surface methodology," *Journal of Environmental Sciences*, vol. 22, no. 8,

pp. 1281–1289, Aug. 2010, doi: 10.1016/S1001-0742(09)60251-5.

[30] S. Chinlee and W. Dechapanya, "COD removal efficiency of pararubber wastewater by ozonation using the central composite design model," *Thai Environmental Engineering Journal*, vol. 36, no. 2, pp. 35-43, May-Aug. 2022.

[31] K. Suwannahong, S. Wongcharee, J. Kreanuarte, and T. Kreetachat, "Pre-treatment of acetic acid from food processing wastewater using response surface methodology via Fenton oxidation process for sustainable water reuse," *Journal of Sustainable Development of Energy, Water and Environment Systems*, vol. 9, no. 4, pp. 1–18, Dec. 2021, doi: 10.13044/j.sdewes.d8.0363.

[32] A. Hadi, A. Niaei, A. Seifi, and Y. Rasoulzadeh, "The impact of operational factors on degradation of formaldehyde as a human carcinogen using Ag_3PO_4/TiO_2 photocatalyst," *Health Promotion Perspectives*, vol. 13, no.1, pp. 47–53, Apr. 2023, doi: 10.34172/hpp.2023.06.

[33] F. Khoshpasand, A. Nikpay, and M. Keshavarz, "Optimization of the photocatalytic oxidation process in toluene removal from air," *Pollution*, vol. 9, no. 2, pp. 567–578, Apr. 2023, doi: 10.22059/POLL.2022.347254.1595.